Journal of Pharmacological Sciences 145 (2021) 279–288

Contents lists available at ScienceDirect

Journal of Pharmacological Sciences

journal homepage: www.elsevier.com/locate/jphs

Full Paper

2,6-DMBQ suppresses cell proliferation and migration via inhibiting mTOR/AKT and p38 MAPK signaling pathways in NSCLC cells

Xiaomeng Xie [a, b], Xueyin Zu [a, b], Kyle Laster [b], Zigang Dong [a, b, c, d, e], Dong Joon Kim [a, b, c, *]

[a] Department of Pathophysiology, School of Basic Medical Sciences, Academy of Medical Science, College of Medicine, Zhengzhou University, Zhengzhou, Henan, 450008, China
[b] China-US (Henan) Hormel Cancer Institute, Zhengzhou, Henan, 450008, China
[c] The Collaborative Innovation Center of Henan Province for Cancer Chemoprevention, Zhengzhou, Henan, 450008, China
[d] The Affiliated Cancer Hospital, Zhengzhou University, Zhengzhou, Henan, 450008, China
[e] International Joint Research Center of Cancer Chemoprevention, Zhengzhou, China

ARTICLE INFO

Article history:
Received 14 September 2020
Received in revised form
31 December 2020
Accepted 5 January 2021
Available online 7 January 2021

Keywords:
2,6-DMBQ
Proliferation
AKT
p38 MAPK
NSCLC cells

ABSTRACT

2,6-Dimethoxy-1,4-benzoquinone (2,6-DMBQ) is the major bioactive compound found in fermented wheat germ extract. Although fermented wheat germ extract has been reported to show anti-proliferative and anti-metabolic effects in various cancers, the anticancer potential and molecular mechanisms exerted by 2,6-DMBQ have not been investigated in non-small cell lung cancer (NSCLC) cells. Here, we report that 2,6-DMBQ suppresses NSCLC cell growth and migration through inhibiting activation of AKT and p38 MAPK. 2,6-DMBQ significantly suppressed anchorage-dependent and independent cell growth. Additionally, 2,6-DMBQ induced G2 phase cell cycle arrest through inhibiting the expression and phosphorylation of cyclin B1 and CDC2, respectively. Furthermore, 2,6-DMBQ strongly suppressed NSCLC cell migration through induction of E-cadherin expression. To determine the molecular mechanism(s) exerted by 2,6-DMBQ upon NSCLC cell lines, various signaling kinases were screened; the results indicate that 2,6-DMBQ strongly inhibits the phosphorylation of AKT and p38 MAPK. Additionally, the growth kinetics of cells treated with an AKT or p38 MAPK inhibitor in combination with 2,6-DMBQ indicate that 2,6-DMBQ suppresses NSCLC cell growth and migration through inhibition of AKT and p38 MAPK. Taken together, our results suggest that 2,6-DMBQ is a potential anticancer reagent against NSCLC cells and could be useful for treating lung cancer patients.

1. Introduction

Lung cancer is the most frequently diagnosed malignant cancer and the leading cause of cancer mortality worldwide.[1,2] The two types of lung cancer are non-small cell lung cancer (NSCLC), which comprises approximately 85% of lung cancer cases, and small cell lung cancer (SCLC).[3] Although clinical advances in prevention and therapeutics against lung cancer have progressed in recent years, the survival rate is still less than 20%.[4] The poor survival of lung cancer patients is due to chemoresistance and the distant metastasis at the time of diagnosis.[5] Therefore, novel approaches to chemotherapy, targeted therapy, and prevention of metastasis are urgently needed.

Signaling pathways that regulate cell growth, cell survival, genomic instability, and angiogenesis are correlated with lung cancer progression and metastatic potential.[6] V-Akt murine thymoma viral oncogene homolog (AKT) is a serine/threonine kinase that regulates cell survival, proliferation and many other biological responses through directly inducing the phosphorylation of downstream substrates.[7] AKT isoforms (AKT1, AKT2 and AKT3) have a high sequence homology in the catalytic domains, but diverge in the hydrophobic motif (HM) domain and the pleckstrin homology (PH) domain.[8] It was recently discovered that the AKT signaling pathway induces epithelial–mesenchymal transition (EMT) and migration through regulating E-cadherin expression.[9] Dual-treatment with EGFR and AKT inhibitors was found to synergistically inhibit tumor growth and promote apoptosis in EGFR-resistant NSCLC models.[10]

* Corresponding author. China-US (Henan) Hormel Cancer Institute, No. 127 Dongming Road, Zhengzhou, Henan, 450008, China. Fax: +86 371 6558 7227.
E-mail address: djkim@hci-cn.org (D.J. Kim).
Peer review under responsibility of Japanese Pharmacological Society.

https://doi.org/10.1016/j.jphs.2021.01.003

The p38 mitogen-activated protein kinase (MAPK) family consists of 4 isoforms (α, -β, -γ and δ) encoded by distinct genes with differences in tissue distribution and substrate specificity.[11] Previously, it was observed that phosphorylated p38 MAPK protein levels are strongly increased in lung cancer tissues compared with normal lung tissues.[12] Additionally, treatment of lung cancer patients with p38 MAPK inhibitors has been shown to suppress lung tumor growth.[13] Therefore, AKT and p38 MAPK pathways might be potential therapeutic targets in lung cancer.

Fermented wheat germ extract has been reported to show preventive and therapeutic activities in various cancer cells.[14,15] 2,6-Dimethoxy-1,4-benzoquinone (2,6-DMBQ), a major bioactive compound of fermented wheat germ extract, is a natural phytochemical present in various plants and can modulate several biological processes including oxidative phosphorylation, electron transport activity, and the inhibition of adipogenesis.[16–18] 2,6-DMBQ has also been reported to exert anti-inflammatory, antibacterial and anti-tumor activities.[19,20] Recently, 2,6-DMBQ was shown to inhibit 3T3-L1 adipocyte differentiation via regulation of AMP-activated protein kinase (AMPK) and mammalian target of rapamycin complex 1 (mTORC1).[19] Our previous study also suggested that 2,6-DMBQ is an mTOR inhibitor that reduces gastric cancer growth.[21] However, the efficacy of 2,6-DMBQ and its potential underlying mechanisms have not been investigated in NSCLC cells. Here, we report that 2,6-DMBQ strongly suppresses NSCLC cell proliferation and migration through inhibiting AKT and p38 MAPK signaling pathways.

2. Materials and methods

2.1. Cell lines

H1299, H1650 and H358 human NSCLC cells were purchased from the Cell Bank of the Chinese Academy of Sciences (Shanghai, China). Cells were cytogenetically tested and authenticated before generating cell stocks. Cells were cultured in RPMI 1640 medium (Biological Industries, Cromwell, CT, USA) supplemented with 10% FBS (Biological Industries) and 1% antibiotic-antimycotic solution (Solarbio, Beijing, China). All cells were maintained at 37 °C in a 5% CO_2 humidified incubator and cultured for a maximum of 8 weeks.

2.2. Reagents and antibodies

2,6-DMBQ was purchased from Shanghai Chemic Industry (Shanghai, China). AKT-I, SB203580 (p38-I) and GSK3β-I were purchased from MedChemExpress (Shanghai, China). Antibodies to detect phosphorylated AKT (S473) (Cat# 4060, 1:1000), p38 MAPK (T180/Y182) (Cat# 9211, 1:1000), MKK3/6 (S189/S207) (Cat# 12280, 1:1000), mTOR (S2481) (Cat# 2974, 1:1000), EGFR (Y1068) (Cat# 2220, 1:1000), GSK3β (S9) (Cat# 5558, 1:1000), -CDC2 (Cat# 9111, 1:1000), total AKT (Cat# 4691, 1:1000), GSK3β (Cat# 12456, 1:1000), -MKK3 (Cat# 8535, 1:1000), -mTOR (Cat# 2972, 1:1000), -ERK1/2 (Cat# 4695, 1:1000), -JAK1 (Cat# 3344, 1:1000), -EGFR (Cat# 2232, 1:1000), -CDC2 (Cat# 77055, 1:1000) and Cyclin B1 (Cat# 12231, 1:1000) were purchased from Cell Signaling Technology (Beverly, MA, USA). The β-actin (Cat# sc-47778, 1:3000) and E-cadherin (Cat# sc-7870, 1:1000) antibodies were purchased from Santa Cruz Biotechnology (Santa Cruz, CA, USA). Phosphorylated JAK1 (Y1022) (Cat# SAB4504446, 1:3000) was purchased from Sigma–Aldrich (St Louis, MO, USA). COX2 (Cat# ab15191, 1:1000) was purchased from Abcam (Chembridge Science Park, Chembridge, UK). Phosphorylated ERK1/2 (T202/Y204) (Cat#700012, 1:1000) was purchased from Thermo Fisher Scientific (Waltham, MA, USA). Goat anti-rabbit IgG (H + L) (Cat# ZB2301, 1:10000) and goat anti-mouse IgG (H + L) (Cat# ZB2305, 1:10000) were purchased from Beijing Zhongshan Jinqiao Biotechnology Co. LTD (Beijing, China).

2.3. Western blotting

Proteins were measured by BCA kit (Solarbio) following the manufacturer's suggested protocol. Proteins were separated by SDS-PAGE and transferred to polyvinylidene difluoride membranes (Amersham Biosciences, Piscataway, NJ, USA). Membranes were then blocked with 5% nonfat dry milk (Solarbio) in TBST (TBS with 1% Tween 20) at room temperature for 1 h. After blocking, the membranes were washed three times with TBST and incubated overnight with appropriate primary antibodies at 4 °C. The next day, the membranes were washed with TBST three times and then incubated with an appropriate horseradish peroxidase–linked secondary antibody for 1 h. The membranes were washed three times with TBST and the immuno-reactive proteins were detected by Thermo Scientific SuperSignal West Pico PLUS Chemiluminescent Substrate (Thermo Fisher Scientific) using the ImageQuant LA S4000 system (GE Healthcare, Piscataway, NJ, USA).

2.4. Cell proliferation assay

Cells were seeded (2×10^3 cells per well) in 96-well plates with 100 μl complete growth medium and incubated for 24 h at 37 °C. Cells were treated with various concentrations of 2,6-DMBQ diluted in 100 μl of complete growth medium for 48 h. After the incubation period, 20 μl of MTT solution (Solarbio) were added to each well and the cells were incubated for an additional 2 h at 37 °C. The cell culture medium was then discarded and replaced with 150 μl of DMSO (Kermel, Tianjin, China). Formazan crystals were dissolved by gentle agitation. Cell proliferation was measured at 570 nm wavelength using a Thermo Multiskan plate-reader (Thermo Fisher Scientific, Waltham, MA, USA). To determine the IC_{50}value of all compounds used within this study, we chose the 72 h MTT result to calculate the half maximal inhibitory concentration using GraphPad Prism 5 (GraphPad Software, San Diego, CA, USA). We used the calculated IC_{50} value of AKT-I or SB203580 or GSK3β-I for co-treatment with 2,6-DMBQ.

2.5. Anchorage-independent cell growth

Cells (8×10^3 per well) suspended in complete growth medium -RPMI 1640 supplemented with 10% FBS and 10 μg/ml gentamycin (Solarbio) were added to 0.3% agar (Becton, Dickinson and Company, NJ, USA) with or without various concentrations of 2,6-DMBQ in a top layer over a base layer of 0.6% agar with or without various concentrations of 2,6-DMBQ. The culture dishes were maintained at 37 °C in a 5% CO_2 incubator for 2 weeks. Colonies were photographed using a wide-field microscope and processed for analysis with the Image-Pro Plus software (v.6) program (Media Cybernetics, Rockville, MD, USA).

2.6. Colony formation assay

Cells were seeded (500 cells per well) in 6-well plates with 2 ml complete growth medium (RPMI 1640 supplemented with 10% FBS and 1% antibiotic-antimycotic solution) and incubated for 24 h. Cells were treated with different concentrations of 2,6-DMBQ in 2 ml of complete growth medium and incubated for 1 week. Cells were stained with 0.5% Coomassie brilliant blue (Solarbio) for 20 min and then imaged.

2.7. Cell cycle analysis

Cells were seeded (8×10^4 cells per dish) into 60 mm culture dishes. After incubation for 24 h, cells were treated with various concentrations of 2,6-DMBQ for 24 h and harvested. Cells were then washed with cold phosphate buffered saline (PBS) and fixed in 1 ml 70% cold ethanol. After rehydration, cells were permeabilized with 0.6% Triton X-100 (Solarbio) and digested with 100 μg/ml RNase A (Solarbio) for 1 h. Cells were subsequently stained with 20 μg/ml propidium iodide (Clontech, Palo Alto, CA, USA) for 15 min before analysis by flow cytometry (Becton, Dickinson and Company, Franklin Lakes, NJ, USA).

2.8. Wound healing assay

Cells were seeded (1×10^5 cells per well) in 6-well plates with 100 μl complete growth medium. After incubation for 24 h, the cells were gently scratched using a plastic micro pipette tip and then washed three times with PBS. Cells were treated with various concentrations of 2,6-DMBQ for 24 h or 48 h. The 6-well plates containing the scratch-wounds were photographed in three different fields of each well. The average width of each scratch-wounds was measured and calculated using ImageJ (National Institutes of Health, Bethesda, MD, USA).

2.9. Migration assay

The lower compartment of transwell chambers (Corning, Bedford, MA, USA) were coated with Matrigel (Becton, Dickinson and Company, NJ, USA) and incubated for 30 min at room temperature under sterile conditions. The lower compartment of each chamber was then filled with 600 μl complete growth medium. Fifty thousand cells suspended in 200 μl complete growth medium with or without 2,6-DMBQ were added to the upper compartment. The chambers were incubated for 24 h at 37 °C in a 5% CO_2 atmosphere. Migrated cells were fixed with methanol (Tianjin Zhiyuan Chemical Reagent Co. LTD, Tianjin, China) and stained with hematoxylin (Baso Diagnostics INC, Zhuhai, China) and eosin (Baso Diagnostics INC) prior to imaging. Photos of the stained cells were analyzed using the Image-Pro Plus software (v.6) program (Media Cybernetics).

2.10. Statistical analysis

All quantitative results are indicated as mean values ± S.D. Statistically significant differences were determined using the Student's t test or by one-way ANOVA ($p < 0.05$). Statistical significance was determined using the Statistical Package for Social Science (SPSS) 21.0 (Xishu software, Shanghai, China).

3. Results

3.1. 2,6-DMBQ suppresses anchorage-dependent and -independent growth of NSCLC cells

2,6-DMBQ is a benzoquinone compound (Fig. 1A). We first investigated whether 2,6-DMBQ could affect the growth of NSCLC cells. Cells were treated with 2,6-DMBQ at different doses and incubated for 48 h and before proliferation was analyzed with an MTT assay. Results indicated that anchorage-dependent growth of NSCLC cells was significantly suppressed by 2,6-DMBQ treatment in a dose-dependent manner (Fig. 1B). Specifically, we observed that 2,6-DMBQ strongly inhibited cell growth in H1299 and H1650 cells compared with H358 cells (Fig. 1B). Furthermore, we investigated whether 2,6-DMBQ could induce cell apoptosis in NSCLC cells. Cells were treated with 2,6-DMBQ for 48 h and then cell apoptosis was analyzed by flow cytometry. Results showed that late cell apoptosis by 2,6-DMBQ was strongly increased in H1299 and H1650 cells, but not H358 cells (Supplemental Fig. 1A and B). Therefore, we used H1299 and H1650 NSCLC cells for further study. We next investigated the effect of 2,6-DMBQ on anchorage-dependent growth (Fig. 1C) and anchorage-independent growth (Fig. 1D) in NSCLC cells using foci formation and soft agar assays, respectively. Results indicated that treatment with 2,6-DMBQ strongly inhibited foci number and anchorage-independent growth relative to untreated controls (Fig. 1C and D).

3.2. 2,6-DMBQ increases G2 phase cell cycle arrest in lung cancer cells

We next performed flow cytometry analysis to determine the effect of 2,6-DMBQ on cell cycle progression after treatment with 2,6-DMBQ for 24 h. The results showed that 2,6-DMBQ significantly increased the fraction of cells in G2 phase (Fig. 2A and B). We also examined whether 2,6-DMBQ could affect the expression levels of G2 phase marker proteins. After treatment with 2,6-DMBQ for 24 h, the expression levels of the G2 phase marker proteins cyclin B1 and phosphorylated CDC2 were detected by Western blotting. Our findings indicated that 2,6-DMBQ treatment strongly inhibited the expression levels of the cyclin B1and phosphorylation of CDC2 in NSCLC cell lines (Fig. 2C).

3.3. 2,6-DMBQ inhibits the migration of NSCLC cells

We next performed a wound healing assay to determine the effect of 2,6-DMBQ on lung cancer cell migration. Cells were scratched using a pipette tip and treated with 2,6-DMBQ for 24 or 48 h prior to visualization under microscope. The results indicated that 2,6-DMBQ significantly suppressed cell migration into the wound area compared with the untreated control cells (Fig. 3A). We next performed a series of transwell migration assays to verify the inhibition of cell migration observed upon treatment with 2,6-DMBQ. Cells were treated with 2,6-DMBQ for 24 or 48 h in the transwell chambers; migrated cells were fixed and counted after each time point. The results of the transwell migration assay experiments showed that 2,6-DMBQ strongly inhibited the number of migrated cells compared with untreated control cells (Fig. 3B). Additionally, we next examined whether 2,6-DMBQ could affect expression of the EMT marker protein, E-cadherin, by Western blotting. Results showed that 2,6-DMBQ strongly induced protein expression of the E-cadherin (Fig. 3C).

3.4. 2,6-DMBQ inhibits AKT and p38 MAPK signaling pathways in NSCLC cells

To examine molecular mechanisms of 2,6-DMBQ, cells were treated with 2,6-DMBQ for 24 h before the expression level of various kinase proteins were analyzed by Western blotting. Results indicated that 2,6-DMBQ suppressed phosphorylation of AKT, GSK3β, p38 MAPK and mTOR proteins in a dose-dependent manner (Fig. 4A and B). However, the expression levels of other related kinase proteins were only marginally affected (Fig. 4A and B).

3.5. Reduction of cell growth and wound healing by 2,6-DMBQ is dependent on the activation of AKT and p38

We next further investigated whether 2,6-DMBQ could affect growth of NSCLC cells through AKT and p38 MAPK signaling. We first examined the effect of AKT (AKT-I) or p38 MAPK inhibitor

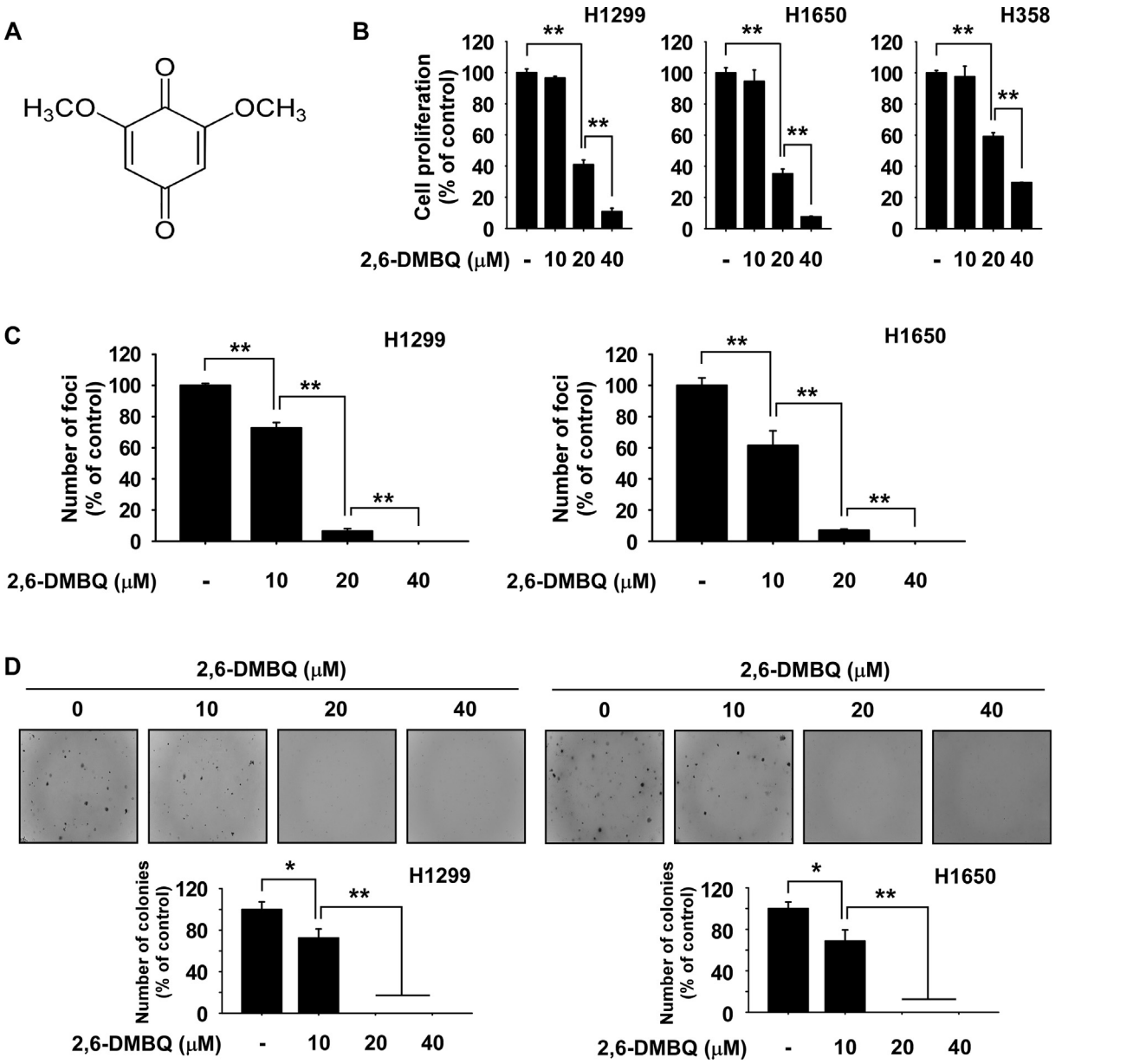

Fig. 1. 2,6-DMBQ inhibits anchorage-dependent and independent growth of NSCLC cells. (A) 2,6-DMBQ is a 2,6-dimethyl-1,4-benzoquinone compound. (B) Effect of 2,6-DMBQ on cell growth. Cells were treated with 2,6-DMBQ at various concentrations for 48 h and growth was determined by the MTT assay. (C) Effect of 2,6-DMBQ on foci formation. Cells were treated with 2,6-DMBQ for 1 week and then colonies were stained and counted. (D) Effect of 2,6-DMBQ on anchorage-independent growth. Cells were treated with 2,6-DMBQ for 2 weeks and then colonies were counted. All data are shown as means ± S.D. of triplicate values from 3 independent experiments and the asterisk (*, **) indicates a significant ($p < 0.05$, $p < 0.01$) difference.

(SB203580) on NSCLC cell growth. The IC_{50} value of the AKT-I (11.9 μM in H1299 and 12.1 μM in H1650) or SB203580 (61.2 μM in H1299 and 80.1 μM in H1650) was first determined by MTT assay (Fig. 5A and B). We next determined how growth of NSCLC cells is affected upon co-treatment with 2,6-DMBQ and AKT-I or SB203580 at the calculated IC_{50} concentration of each inhibitor. Results showed that AKT-I or SB203580-treated cells exhibited increased proliferation compared to 2,6-DMBQ treated cells, suggesting that AKT and p38 MAPK signaling may be required for 2,6-DMBQ-mediated growth inhibition (Fig. 5C and D). Additionally, we also investigated the effect of combining 2,6-DMBQ with AKT-I or SB203580 at their respective IC_{50} concentrations on wound healing of NSCLC cells. Results indicated that co-treatment with either inhibitor in conjunction with 2,6-DMBQ did not significantly alter the rate of migration compared with cells treated with 2,6-DMBQ treatment alone (Fig. 6A and B). Furthermore, we examined whether 2,6-DMBQ could regulate cell growth or wound healing of NSCLC cells through GSK3β protein. Cells were treated with GSK3β inhibitor (GSK3β-I) at the IC_{50} concentration (Supplemental Fig. 2A) in the presence or absence of 2,6-DMBQ. Results indicated that the cell growth of co-treated H1299 cells were suppressed compared to 2,6-DMBQ treatment alone; however, the growth of co-treated H1650 cells was only marginally affected (Supplemental Fig. 2B). Additionally, co-treatment with GSK3β-I and 2,6-DMBQ did not significantly impair wound healing in either NSCLC cell line relative to cells treated with 2,6-DMBQ alone (Supplemental Fig. 2C).

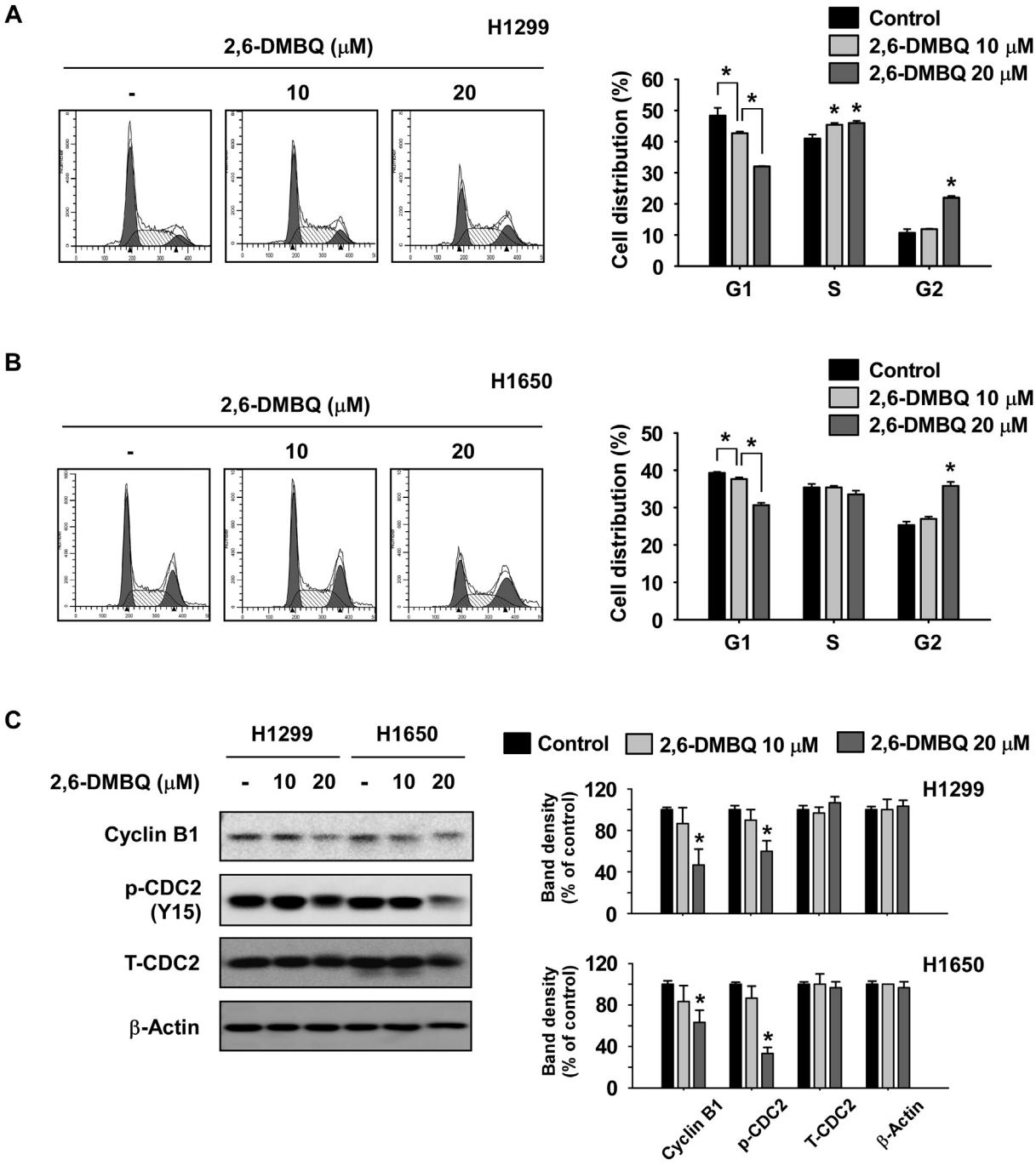

Fig. 2. 2,6-DMBQ induces G2 phase cell cycle arrest in NSCLC cells. Effect of 2,6-DMBQ on cell cycle in H1299 (A) and H1650 (B) NSCLC cells. Cells were treated with 2,6-DMBQ for 24 h in complete growth medium and stained with propidium iodide (PI). Cell cycle was measured by Fluorescence Activated Cell Sorting (FACS). For A and B, data are shown as means ± S.D. of triplicate values from 3 independent experiments and the asterisk (*) indicates a significant ($p < 0.05$) difference. (C) Effect of 2,6-DMBQ on the expression of G2 phase cell cycle marker proteins was analyzed by Western blotting. Band density was measured using the Image J (NIH) software program. Similar results were observed from 3 independent experiments and as a bar graph.

4. Discussion

Fermented wheat germ extract has been reported to show cancer preventive and therapeutic effects.[22,23] Notably, fermented wheat germ extract is clinically used as a non-prescription medical nutriment for cancer patients. Therefore, it is of great scientific and clinical significance to explore its underlying mechanism. 2,6-DMBQ, as a bioactive compound from fermented wheat germ extract, has been reported to show preventive effects on the promotion and initiation stages of mouse skin tumorigenesis.[24] 2,6-DMBQ induced oxidative stress-mediated cytotoxicity in human cancer cell lines.[25] In our previous study, we suggested that 2,6-DMBQ inhibited gastric cancer cell growth by modulating the mTOR signaling pathway.[25] When the effect of 2,6-DMBQ on gastric cancer cells depleted of mTOR was assessed, the results indicated that cells expressing reduced levels of mTOR were resistant to the inhibitory effect of 2,6-DMBQ compared to cells expressing wild-type levels of mTOR. Therefore, we also investigated whether 2,6-

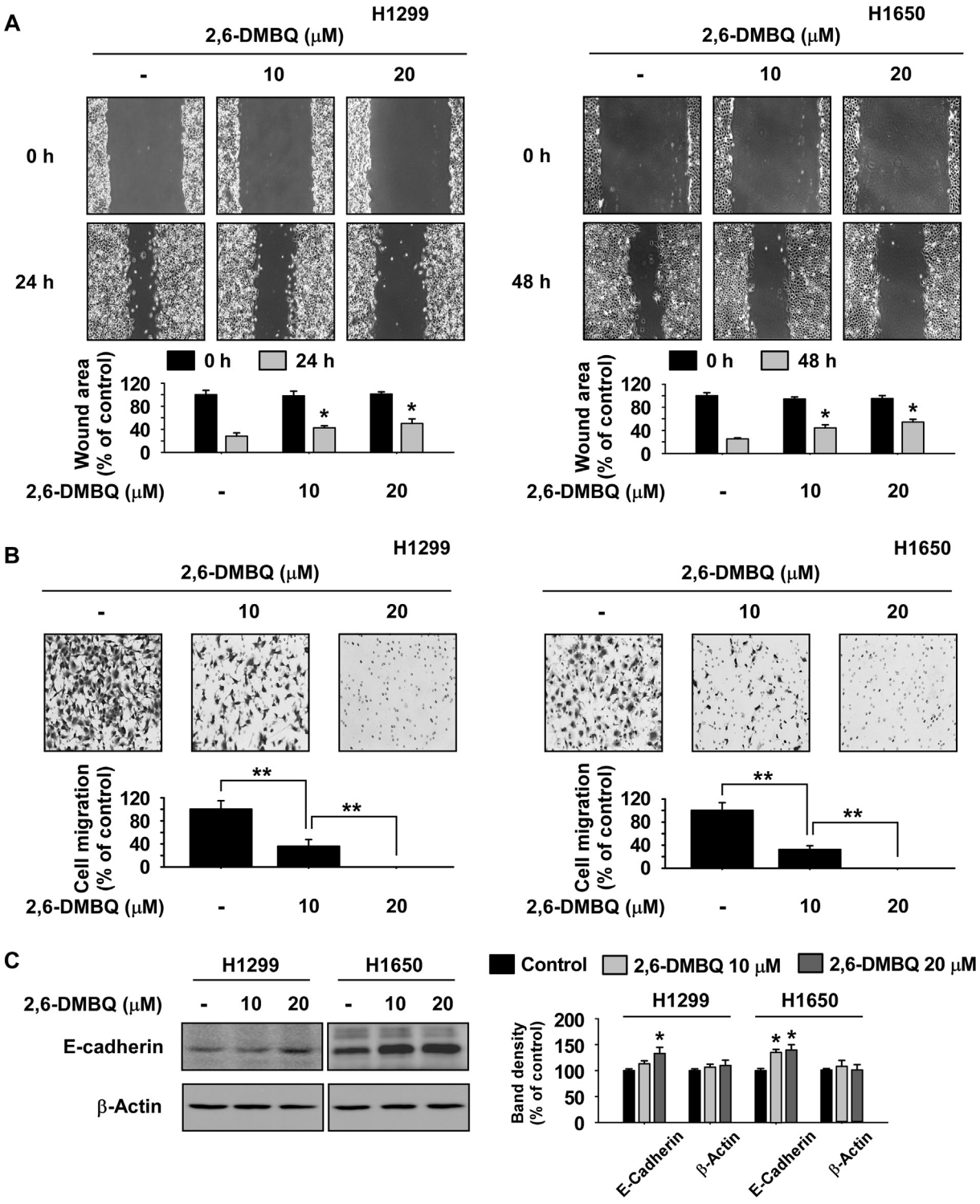

Fig. 3. 2,6-DMBQ inhibits cell migration through regulating the expression of EMT marker protein in NSCLC cells. (A) Effect of 2,6-DMBQ on wound healing ability. Cells were scratched and treated with 2,6-DMBQ for 24 or 48 h. Similar results were observed from 3 independent experiments. (B) Effect of 2,6-DMBQ on cell migration. Cells were seeded and treated with 2,6-DMBQ for 24 h in transwells. Migrated cells were counted. Data are shown as means ± S.D. of triplicate values from 3 independent experiments and the asterisk (*) indicates a significant difference ($p < 0.05$). (C) Effect of 2,6-DMBQ on the expression of EMT marker protein. Band density was measured using the Image J (NIH) software program and similar results were observed from 3 independent experiments and as a bar graph.

DMBQ could affect growth or would healing of NSCLC cells through mTOR signaling. Results indicated that NSCLC cells depleted of mTOR through shRNA were resistant to the inhibitory effect of 2,6-DMBQ with respect to cell growth and wound healing compared to 2,6-DMBQ-treated shControl cells (Supplemental Fig. 3A–C). However, a high dose of 2,6-DMBQ still showed a strong effect on shmTOR gastric and NSCLC cancer cells. Therefore, we suggest that it is highly likely that 2,6-DMBQ has additional molecular targets.

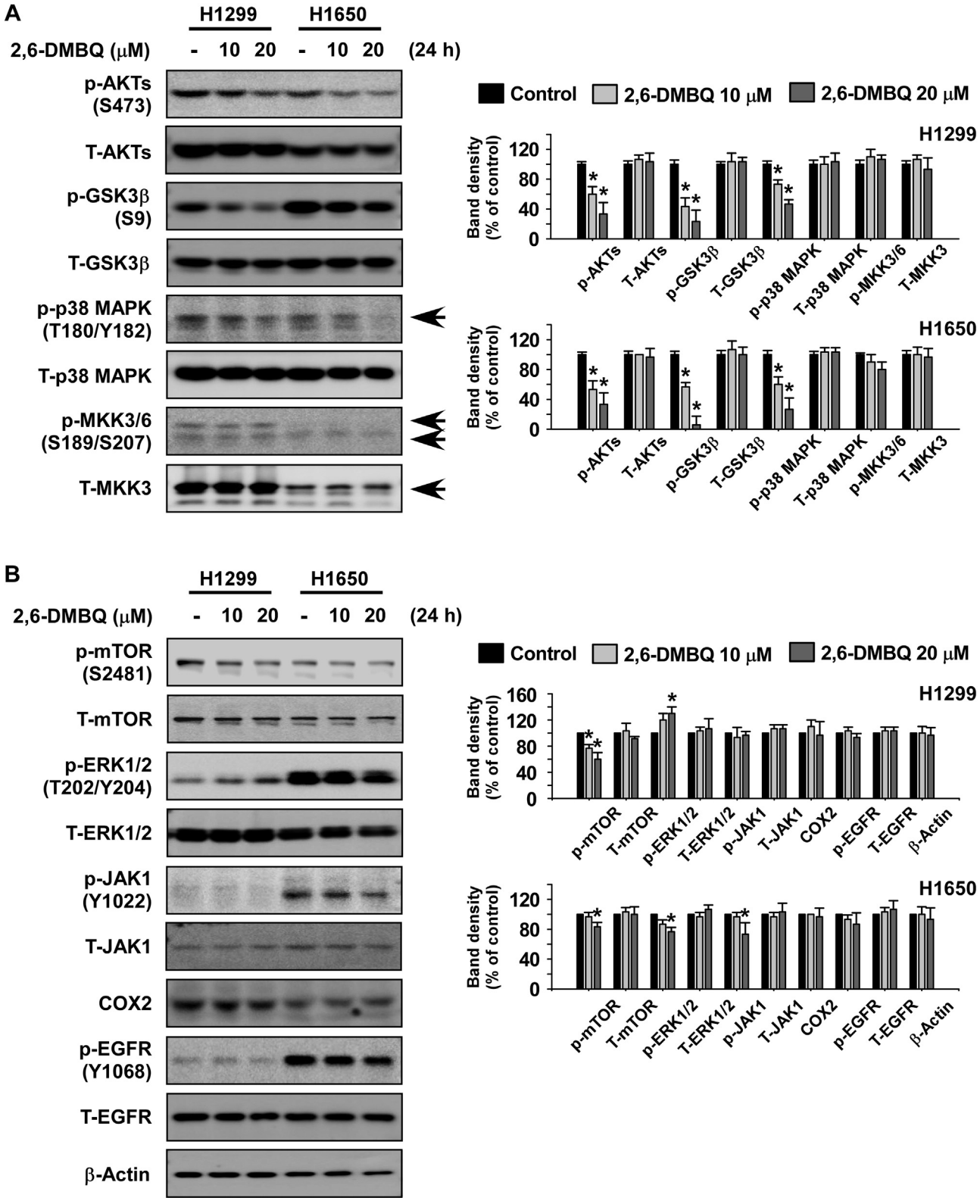

Fig. 4. 2,6-DMBQ inhibits AKT and p38 MAPK signaling pathways in NSCLC cells. (A, B) Effect of 2,6-DMBQ on kinase signaling pathways. Cells were treated with 2,6-DMBQ for 24 h and then various kinase proteins were examined by Western blotting. Band density was measured using the Image J (NIH) software program. Similar results were observed from 3 independent experiments and as a bar graph. All data are shown as means ± S.D. from 3 independent experiments and the asterisk (*) indicates a significant ($p < 0.05$) difference.

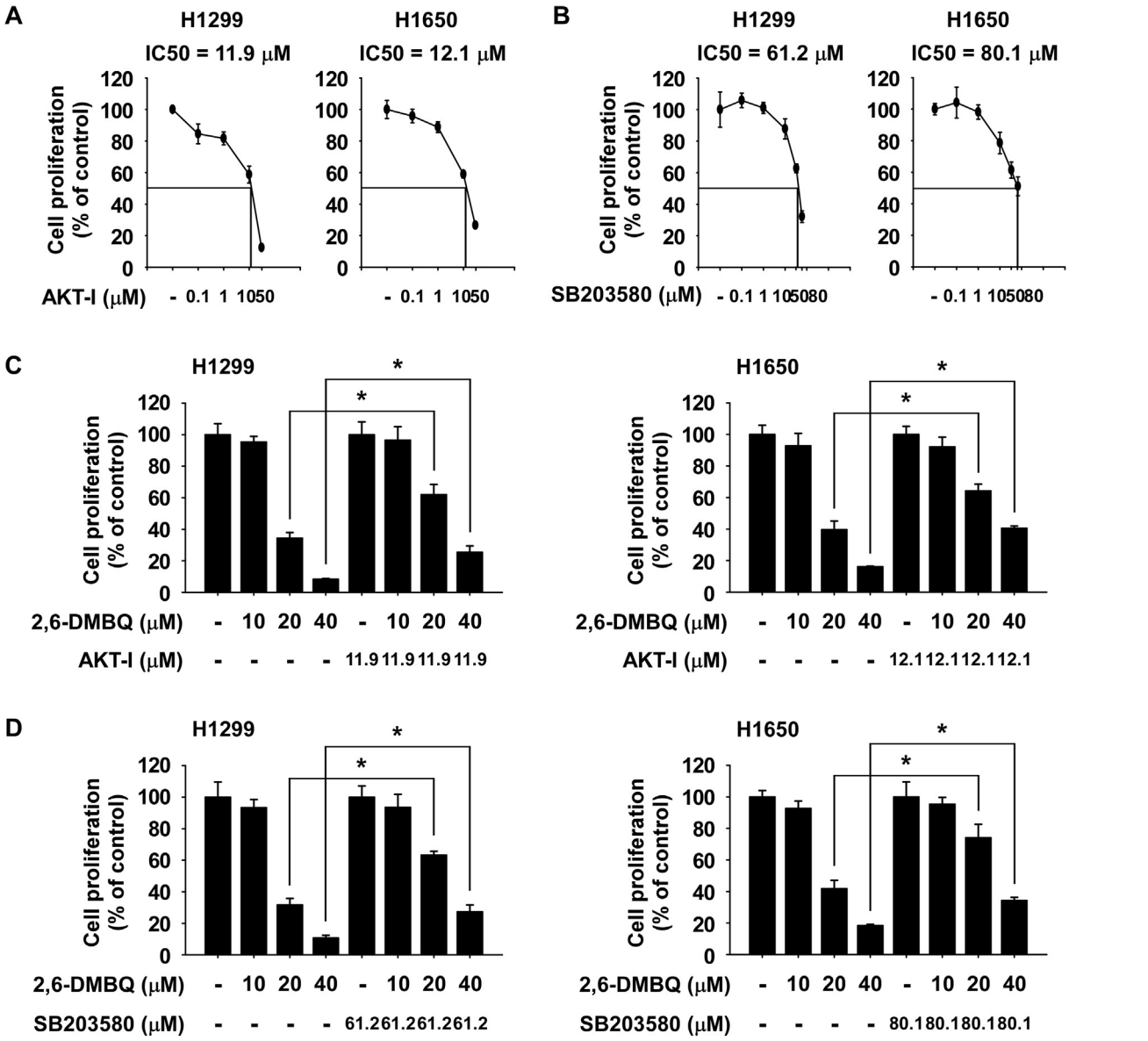

Fig. 5. Reduction of cell growth by 2,6-DMBQ is dependent on the activation of AKT and p38 MAPK. (A, B) IC_{50} value of AKT inhibitor (AKT-I) and p38 inhibitor (SB203580). Cells were treated with various concentrations of AKT-I or SB203580 for 72 h. IC_{50} value was determined by the MTT assay. Effect of 2,6-DMBQ combined with AKT-I (C) or SB203580 (D) on cell growth. Cells were treated with 2,6-DMBQ combined with or without AKT-I or SB203580 at various concentrations for 48 h. Cell growth was determined by the MTT assay. All data are shown as means ± S.D. of triplicate values from 3 independent experiments and the asterisk (*) indicates a significant ($p < 0.05$) difference.

Additionally, 2,6-DMBQ showed anti-tumor activity in NSCLC cells in the present study. Therefore, we further characterized 2,6-DMBQ in identifying additional potential molecular targets.

AKT1 is mainly involved in cellular invasion, while AKT2 promotes cell proliferation, colony formation and tumor growth.[26] Additionally, phosphorylated AKT is strongly overexpressed in NSCLC tissues compared with normal lung tissues and highly correlated with a shorter survival rate.[27] Inhibition of AKT activity by an AKT inhibitor or dominant negative mutant form of AKT has been observed to induce G2 phase cell-cycle arrest.[28,29] Moreover, inhibition of AKT signaling has been shown to decrease the expression of cyclin B1 and CDC2.[30–32] Therefore, we provided evidence suggesting that 2,6-DMBQ strongly induced G2 phase cell cycle arrest and reduced the expression of cyclin B1 and phosphorylation of CDC2 through its inhibition of AKT activity (Fig. 2A–C).

EMT is a dynamic cellular process that affects various biological properties of malignant tumors.[33] Our results suggest that 2,6-DMBQ inhibited cell migration of NSCLC and the expression of EMT marker protein through suppressing AKT and p38 MAPK signaling pathways (Fig. 3A–C, Fig. 4A). It has been previously reported that activation of AKT signaling pathways can promote the EMT process,[34,35] which facilitates chemoresistance against epidermal growth factor receptor (EGFR) inhibitors in lung cancer.[36] Additionally, the phosphorylation of p38 MAPK protein is increased in lung tumor tissues compared with normal lung tissues.[37] Selective p38 MAPK inhibitor treatment has been found to induce the expression of E-cadherin.[38] Interestingly, inhibition of EMT showed benefit when used in combination with standard chemotherapies or targeted therapies in NSCLC.[39] Therefore, it is an urgent task to identify inhibition of EMT for improving anticancer drug efficacy in the context of lung cancer. We strongly suggest 2,6-

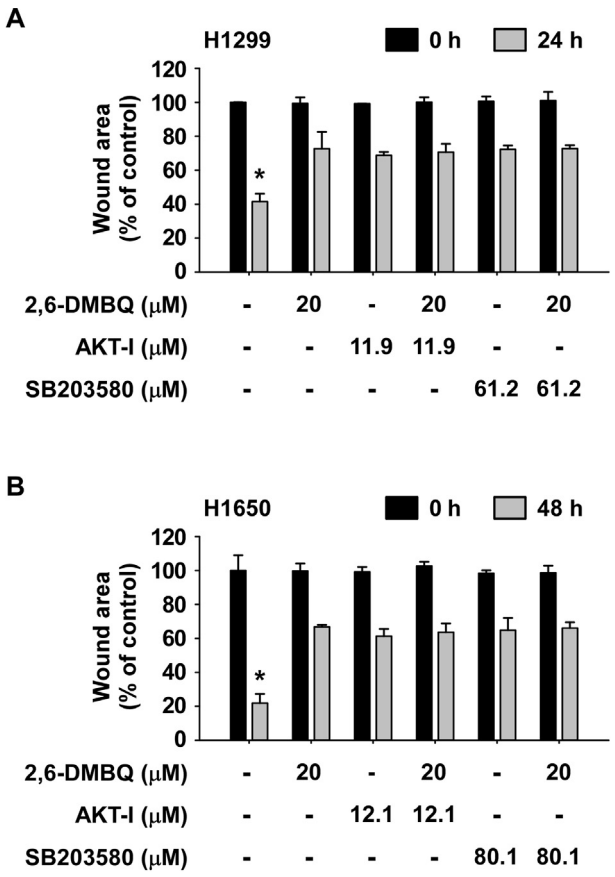

Fig. 6. Inhibition of wound healing by 2,6-DMBQ is dependent on the activation of AKT and p38 MAPK. (A, B) Effect of 2,6-DMBQ combined with AKT inhibitor (AKT-I) or p38 MAPK inhibitor (SB203580) on wound healing in H1299 (A) and H1650 NSCLC cells (B). Cells were scratched and treated with 2,6-DMBQ combined with or without AKT-I or SB203580 at various concentrations. Similar results were observed from 3 independent experiments and as a bar graphand the asterisk (*) indicates a significant ($p < 0.05$) difference.

DMBQ as a candidate that may be combined with EGFR inhibitors to overcome chemoresistance; this novel combination regimen could be useful for NSCLC treatment.

In conclusion, this study has suggested that 2,6-DMBQ suppresses NSCLC cell proliferation and migration via regulating AKT and p38 MAPK signaling pathways. Furthermore, we are planning subsequent studies to further characterize other potential molecular targets of 2,6-DMBQ in order to elucidate additional toxicological responses.

Declaration of competing interest

None of the authors have any competing interests.

Acknowledgements

Not applicable.

Appendix A. Supplementary data

Supplementary data to this article can be found online at https://doi.org/10.1016/j.jphs.2021.01.003.

Funding

This work was supported by the Henan Joint Fund, National Natural Science Foundation China (NSFC), China [grant number U1804196 and 82073075] and Youth Science Foundation of Natural Science Foundation of Henan Province, China [grant number 212300410315].

Availability of data and materials

None.

Authors' contributions

X.X. performed the cell-based experiments and prepared the manuscript; X.Z assisted with the cell-based assays; K.L assisted with data analysis and editing the manuscript; Z.D. supervised the overall experimental design; D.J.K. supervised the overall experimental design and provided the idea and manuscript editing.

References

1. Torre LA, Bray F, Siegel RL, Ferlay J, Lortet-Tieulent J, Jemal A. Global cancer statistics, 2012. *CA A Cancer J Clin*. 2015;65(2):87–108.
2. Molina JR, Yang P, Cassivi SD, Schild SE, Adjei AA. Non-small cell lung cancer: epidemiology, risk factors, treatment, and survivorship. *Mayo Clin Proc*. 2008;83(5):584–594.
3. Bray F, Ferlay J, Soerjomataram I, Siegel RL, Torre LA, Jemal A. Global cancer statistics 2018: GLOBOCAN estimates of incidence and mortality worldwide for 36 cancers in 185 countries. *CA A Cancer J Clin*. 2018;68(6):394–424.
4. Torre LA, Siegel RL, Jemal A. *Lung cancer statistics*893. 2016:1–19.
5. Herbst RS, Morgensztern D, Boshoff C. The biology and management of non-small cell lung cancer. *Nature*. 2018;553(7689):446–454.
6. Perlikos F, Harrington KJ, Syrigos KN. Key molecular mechanisms in lung cancer invasion and metastasis: a comprehensive review. *Crit Rev Oncol Hematol*. 2013;87(1):1–11.
7. Song M, Bode AM, Dong Z, Lee MH. AKT as a therapeutic target for cancer. *Canc Res*. 2019;79(6):1019–1031.
8. Manning BD, Toker A. AKT/PKB signaling: navigating the network. *Cell*. 2017;169(3):381–405.
9. Karimi Roshan M, Soltani A, Soleimani A, Rezaie Kahkhaie K, Afshari AR, Soukhtanloo M. Role of AKT and mTOR signaling pathways in the induction of epithelial-mesenchymal transition (EMT) process. *Biochimie*. 2019;165:229–234.
10. Jacobsen K, Bertran-Alamillo J, Molina MA, et al. Convergent Akt activation drives acquired EGFR inhibitor resistance in lung cancer. *Nat Commun*. 2017;8(1):410.
11. Johnson GL, Lapadat R. Mitogen-activated protein kinase pathways mediated by ERK, JNK, and p38 protein kinases. *Science*. 2002;298(5600):1911–1912.
12. Greenberg AK, Basu S, Hu J, et al. Selective p38 activation in human non-small cell lung cancer. *Am J Respir Cell Mol Biol*. 2002;26(5):558–564.
13. Campbell RM, Anderson BD, Brooks NA, et al. Characterization of LY2228820 dimesylate, a potent and selective inhibitor of p38 MAPK with antitumor activity. *Mol Canc Therapeut*. 2014;13(2):364–374.
14. Zhang K, Dai H, Liang W, Zhang L, Deng Z. Fermented dairy foods intake and risk of cancer. *Int J Canc*. 2019;144(9):2099–2108.
15. Mueller T, Jordan K, Voigt W. Promising cytotoxic activity profile of fermented wheat germ extract (Avemar(R)) in human cancer cell lines. *J Exp Clin Canc Res*. 2011;30:42.
16. Sanchez-Cruz P, Garcia C, Alegria AE. Role of quinones in the ascorbate reduction rates of S-nitrosoglutathione. *Free Radic Biol Med*. 2010;49(9):1387–1394.
17. Drewes SE, Khan F, van Vuuren SF, Viljoen AM. Simple 1,4-benzoquinones with antibacterial activity from stems and leaves of Gunnera perpensa. *Phytochemistry*. 2005;66(15):1812–1816.
18. Koyama J. Anti-infective quinone derivatives of recent patents. *Recent Pat Anti-Infect Drug Discov*. 2006;1(1):113–125.
19. Son HJ, Jang YJ, Jung CH, Ahn J, Ha TY. 2,6-Dimethoxy-1,4-benzoquinone inhibits 3T3-L1 adipocyte differentiation via regulation of AMPK and mTORC1. *Planta Med*. 2019;85(3):210–216.
20. Jeong HY, Choi YS, Lee JK, Lee BJ, Kim WK, Kang H. Anti-inflammatory activity of citric acid-treated wheat germ extract in lipopolysaccharide-stimulated macrophages. *Nutrients*. 2017;9(7).
21. Zu X, Ma X, Xie X, et al. 2,6-DMBQ is a novel mTOR inhibitor that reduces gastric cancer growth in vitro and in vivo. *J Exp Clin Canc Res*. 2020;39(1):107.

22. Telekes A, Hegedus M, Chae CH, Vekey K. Avemar (wheat germ extract) in cancer prevention and treatment. *Nutr Canc*. 2009;61(6):891–899.
23. Hidvegi M, Raso E, Tomoskozi-Farkas R, Paku S, Lapis K, Szende B. Effect of Avemar and Avemar + vitamin C on tumor growth and metastasis in experimental animals. *Anticancer Res*. 1998;18(4A):2353–2358.
24. Kamiya T, Tanimoto Y, Fujii N, et al. 2,6-Dimethoxy-1,4-benzoquinone, isolation and identification of anti-carcinogenic, anti-mutagenic and anti-inflammatory component from the juice of Vitis coignetiae. *Food Chem Toxicol*. 2018;122:172–180.
25. Otto C, Hahlbrock T, Eich K, et al. Antiproliferative and antimetabolic effects behind the anticancer property of fermented wheat germ extract. *BMC Compl Alternative Med*. 2016;16:160.
26. Attoub S, Arafat K, Kamel Hammadi N, Mester J, Gaben AM. Akt2 knockdown reveals its contribution to human lung cancer cell proliferation, growth, motility, invasion and endothelial cell tube formation. *Sci Rep*. 2015;5:12759.
27. Tang JM, He QY, Guo RX, Chang XJ. Phosphorylated Akt overexpression and loss of PTEN expression in non-small cell lung cancer confers poor prognosis. *Lung Canc*. 2006;51(2):181–191.
28. Song M, Liu X, Liu K, et al. Targeting AKT with oridonin inhibits growth of esophageal squamous cell carcinoma in vitro and patient-derived xenografts in vivo. *Mol Canc Therapeut*. 2018;17(7):1540–1553.
29. Lee SR, Park JH, Park EK, Chung CH, Kang SS, Bang OS. Akt-induced promotion of cell-cycle progression at G2/M phase involves upregulation of NF-Y binding activity in PC12 cells. *J Cell Physiol*. 2005;205(2):270–277.
30. Lin W, Xie J, Xu N, et al. Glaucocalyxin A induces G2/M cell cycle arrest and apoptosis through the PI3K/Akt pathway in human bladder cancer cells. *Int J Biol Sci*. 2018;14(4):418–426.
31. Liu JS, Huo CY, Cao HH, et al. Aloperine induces apoptosis and G2/M cell cycle arrest in hepatocellular carcinoma cells through the PI3K/Akt signaling pathway. *Phytomedicine*. 2019;61:152843.
32. Zhao L, Miao HC, Li WJ, et al. LW-213 induces G2/M cell cycle arrest through AKT/GSK3beta/beta-catenin signaling pathway in human breast cancer cells. *Mol Carcinog*. 2016;55(5):778–792.
33. Zhu X, Chen L, Liu L, Niu X. EMT-mediated acquired EGFR-TKI resistance in NSCLC: mechanisms and strategies. *Front Oncol*. 2019;9:1044.
34. Tang Z, Ding Y, Shen Q, et al. KIAA1199 promotes invasion and migration in non-small-cell lung cancer (NSCLC) via PI3K-Akt mediated EMT. *J Mol Med (Berl)*. 2019;97(1):127–140.
35. Meng J, Zhang XT, Liu XL, et al. WSTF promotes proliferation and invasion of lung cancer cells by inducing EMT via PI3K/Akt and IL-6/STAT3 signaling pathways. *Cell Signal*. 2016;28(11):1673–1682.
36. Tulchinsky E, Demidov O, Kriajevska M, Barlev NA, Imyanitov E. EMT: a mechanism for escape from EGFR-targeted therapy in lung cancer. *Biochim Biophys Acta Rev Canc*. 2019;1871(1):29–39.
37. Igea A, Nebreda AR. The stress kinase p38alpha as a target for cancer therapy. *Canc Res*. 2015;75(19):3997–4002.
38. Lin Y, Mallen-St Clair J, Wang G, et al. p38 MAPK mediates epithelial-mesenchymal transition by regulating p38IP and Snail in head and neck squamous cell carcinoma. *Oral Oncol*. 2016;60:81–89.
39. Du B, Shim JS. Targeting epithelial-mesenchymal transition (EMT) to overcome drug resistance in cancer. *Molecules*. 2016;21(7):965–980.